Preparation and Performance of Modified Montmorillonite-reinforced Wood-based Foamed Composites

Qingde Li,[a] Yingyi Liang,[b] Feng Chen,[c,*] and Tonghui Sang [d]

Wood fiber was modified by impulse-cyclone drying treatment with poplar and montmorillonite as reinforcing materials; mMMT/polypropylene/wood fiber foaming composite was prepared by the hot compression process. The effects of modification, temperature, and content of montmorillonite on physical and mechanical properties of the composite were analyzed. Mechanical properties, porosity, shrinkage, water absorption, and thickness swelling tests showed that when mMMT reinforcement was 5 wt%, the best performance was achieved. The scanning electron microscopy observations showed that bubble holes were distributed widely and evenly, and mMMT appeared in the cell gap and was encapsulated by polypropylene, which maximized the bonding effect. Flexural strength was 27.5 MPa, flexural modulus was 2110 MPa, tensile strength was 20.0 MPa, and impact strength was 6.30 KJ/m^2. When absolute volume of dense solid reached 70.8 cm^3, porosity was 21.4% and shrinkage was 1.17%, which indicated that the water absorption increased most remarkably under that test condition. When equilibrium water absorption reached 9.28%, the thickness swelling decreased by 25%. The results showed that mMMT effectively optimized mechanical properties of wood-based foamed composites and improved hygroscopic properties.

*Contact information: a: School of Industrial Design and Ceramic Art, Foshan University, Foshan 528225, China; b: School of Medical Engineering, Foshan University, Foshan 528225, China; c: School of Art and Design, Taizhou University, Taizhou 318000, China; d: Faculty of Music and Performing Arts, Universiti Malaysia Kelantan, City Campus, Locked Bag 36, 16100 Pengkalan Chepa, Kota Bharu, Kelantan, Malaysia; *Corresponding author: 47893729@qq.com*

INTRODUCTION

Wood-based foamed composite (WFCs) material is based on the basic formula of wood-based composite material that is mixed with a foamer, nucleating agent, foaming auxiliary agent, and so on in a certain proportion of mass. This material is also heated and melted by plastic molding equipment to become a type of composite material with continuous and uniform distribution of foamed micropores (Wang *et al.* 2019). The industry of wood-based foam composites has developed rapidly in the past two decades (Kallakas *et al.* 2019). Wood fiber is a strong filling material (Yang *et al.* 2004; Gamelas and Ferraz 2015). The organic components in fiber are mainly cellulose, hemicellulose, and lignin, which lead to many shortcomings of WFCs, such as low ductility, low strength, poor internal bonding strength, and high density (Zhang *et al.* 2004; Wang *et al.* 2005; Choi *et al.* 2006).

Adding a foamer can effectively optimize the properties of composites, such as reducing material consumption and improving surface hydrophobicity (Han *et al*. 2011). The use of foamer can also effectively reduce the weight and density of WPCs and improve mechanical properties. Therefore, it is important to add foamer in the process of wood-based composites.

Bledzki and Faruk found that the foamer could effectively reduce surface roughness of WPC by nearly 70% (Bledzki and Faruk 2006). Matuana *et al.* (1997) found that cell morphology and quantity of foamed polyvinyl chloride (PVC)/wood fiber composite depended on the amount of plasticizer, surface treatment of wood fiber, gas saturation, and foaming conditions. Petchwattana's study concluded that when the size of foam hole increases, compressive and tensile strength of foamed composites decreases (Petchwattana and Covavisaruch 2011). Babaei *et al.* (2014) modified nanoclay with azodicarbonamide and then prepared foamed modified nanoclay/high-density polyethylene (HDPE)/wheat straw powder (WSP) composites using injection molding machines. The results showed that average pore size decreased 21.7% with the increase of pore density *via* addition of 200% to 400% modified nano-clay, and pore size further decreased with the increase of pore density when reinforcements reached 500%. When the amount of modified nanoclay increased from 0% to 400%, the water absorption increased to 19.3% and thickness swelling of samples was increased to 26.5%, respectively. Mechanical properties of HPDE/WSF composite materials became optimal when two parts of modified nanoclay were added. It should also be noted that reinforcement of modified nanomaterials has a great negative impact on impact resistance of foamed composites (Babaei *et al*. 2014).

To improve physical and mechanical properties of foamed composites and uniformity of foaming, it is necessary to modify wood fiber to reduce its polarity. Common methods are chemical modification represented by alkali treatment, acylation, and graft copolymerization, and physical modification, represented by high temperature heat treatment and microwave treatment. Drying pretreatment of biomass is a common, effective, and environmentally friendly modification method. Impulse-cyclone drying treatment modification has the advantages of lower cost, shorter time, higher strength, a simpler process, and so on, which can degrade the wood fiber chemical composition. Hemicelluloses with poor thermal stability degrade first, and molecular chain fracture may occur in the process of degradation, and even lignin and cellulose microfibril may also break (Ding *et al*. 2019; Jonasson *et al*. 2019), which may lead to roughened wood fiber surface, enhanced depth to resin in high temperature mixed diffusion, and improved mechanical interlock ability. Impulse-cyclone drying treatment can also greatly reduce the number of free hydroxyl groups in wood fiber components, reduce polarity (Yu *et al*. 2020), and improve crystallinity of cellulose (Gao *et al*. 2019), so as to improve compatibility between the wood fiber and plastic matrix and improve dimensional stability (Okon and Udoakpan 2019) and mechanical properties of wood composites (Sun and Wu 2019).

In this study, cottonwood fiber and montmorillonite were used as reinforcing materials to modify wood fiber with an impulse-cyclone drying treatment. With wood-based foaming composites prepared by high temperature treatment, the influences of mMMT (modified montmorillonite) and foamer ADC (foamer azodicaramide) on properties of wood-based foaming composites were investigated.

EXPERIMENTAL

Materials

The foamer azodicaramide (foamer ADC) was purchased from Shanghai Kamesh Biotechnology Co., Ltd. (Shanghai, China). Polypropylene (PP) was purchased from CNPC Daqing Petroleum Chemical Industrial Factory (Daqing, China). Leftovers of poplar were provided by Zhongshan Yong Xu Wood-Based Panel Company (Zhongshan, China). Maleic anhydride grafted polyethylene (MAPE) was purchased from Guangzhou Bai Chen Co., Ltd. (Guangzhou, China). Dryers, montmorillonite (MMT), Na_2SO_4, and vaseline were all purchased from Tianjin Benchmark Chemical Reagent Co., Ltd. (Tianjin, China).
The MMT and silane coupling agent were provided Zhejiang Feidian Chemical Co., Ltd., (Hangzhou, China).

Methods

Preparation of modified montmorillonite/polypropylene/wood fiber foamed composites

Poplar leftovers were processed into 40-mesh > 60-mesh wood fiber using a 60-type wood fiber mill (Xingtai Maple Machinery Manufacturing Co., Ltd., Hebei, China), and placed in the forced convection constant temperature drying oven (101A-4HA; Shanghai Kanglu Instrument Equipment Co., Ltd., Shanghai, China) at 103 °C and dried to a moisture content of less than 3%.

MMT and silane coupling agent were purchased from Zhejiang Feidian Chemical Co., Ltd. The structural formula of MMT is $(Al, Mg)_2 [Si_4O_{10}] (OH)_2 \cdot n\ H_2O$. The MMT was dried to a moisture content of below 3%, ground and screened using an 80 mesh sieve. The silane coupling agent (KH-550: $NH_2CH_2CH_2CH_2Si(OC_2H_5)_3$) had a boiling point of 217 °C. The MMT was mixed with silane coupling agent at a mass ratio of 100:4, fully mixed in a high-speed mixer with a temperature of 60 °C (GHV type; Tianjin Saide Electric Control Mechanical Equipment Co., Ltd., Tianjin, China), and then dried at 80 °C for 6 h to obtain mMMT. There were two functional groups in the silane coupling agent. One was reacted with hydroxyl group, and the other underwent a chemical reaction with functional groups in the plastic, or physical mixing with the polymer matrix was achieved, so that MMT and wood fiber were effectively linked together.

Impulse-cyclone drying (ICD) treatment has a short treatment time, high intensity, high efficiency, a simple process, and it is environmentally friendly. Wood fibers were first subjected to high-temperature hot air, which was generated using a heat generator, a screw feeder, an induced draft fan at a temperature of 220 °C, an inlet air velocity of 10 m/s, and a feed rate of 120 kg/h. The wood fiber was placed in a multi-function high temperature and high pressure water vapor treatment device generator with a temperature of 220 °C and a pressure of 0.6 MPa for modification treatment, and the treatment time was 15 min. Then it was placed in a constant temperature and humidity drying box under the condition of 105 °C, and the moisture content of the wood fiber was dried to 3%. Wood fiber, PP (T30S, Melt Indexer 2-3 g/10 min), MAPE (PE-12, HDPE: MAH=100:1.5, 190 °C, 2.16 kg, melt indexer 1 to 4 g/10 min), lubricant (paraffin), mMMT, and foamer ADC were prepared according to the test piece ratio scheme and placed at room temperature. In a high-mixing machine, they were stirred and mixed for 15 min at high speed, made uniform, and then placed in the twin-screw extruder of SJSH30/SJ45 double-stage plastic extrusion unit (Yuyao Ludao Rubber & Plastic

Machinery Co., Ltd., Yuyao, China) for granulation. They were prepared by hot pressing at a high temperature using a PP 600D hot press machine (JingTuo Instrument Technology Co., Ltd., Tianjin, China). Paraffin was used as a lubricant, mMMT was used as an enhancer, and ADC was used as a foamer in this experiment. The specific formula is shown in Table 1. The specific experimental process is as follows.

White wood residue → wood powder → drying
PP, MAPE and paraffin additives
mMMT   → high speed mixing → double
Foamer ADC   screw extrusion granulation →
Extrusion   hot press molding

Extrusion molding process conditions were that the extruder screw tube temperature was between 145 °C to 170 °C, head temperature of 165 °C, host frequency was 22 Hz, feeding speed of 45 r/min, and cutting speed of 356 r/min. The temperature settings of the twin screw extruder were 160 °C in zone 1, 165 °C in zone 2, 170 °C in zone 3, 170 °C in zone 4, 185 °C in zone 5, 170 °C in zone 6, and 165 °C in zone 7. The speed of the extruder was set at 60 rpm. The prepared raw material particles were hot-pressed using a zs-406b electric sulfur-adding molding machine (Zhuosheng Mechanical Equipment Co., Ltd., Dongwan, China). The temperature was set at 180 °C, prepressed for 15 min, hot-pressed for 10 min under 5 MPa, and cold-pressed for 5 min. The thickness of the test piece was 4 mm. The prepared mMMT/PP/wood fiber foamed composites were then prepared into standard samples using an electric saw and dumbbell-type sample-making machine (Hongrui Precision Cutting Tools Co., Ltd., Dongwan, China). Finally, the modified montmorillonite reinforced wood-based foamed composite samples were prepared.

Table 1. Composition of Sample of Wood-based Foaming Composites

Sample No.	PP	Wood Fiber	MAPE	Paraffin	Foamer ADC	mMMT
1	67%	27%	3%	1%	2%	0%
2	67%	27%	3%	1%	2%	3%
3	67%	27%	3%	1%	2%	5%
4	67%	27%	3%	1%	2%	7%
5	67%	27%	3%	1%	2%	10%

Note: The total amount of PP, wood fiber, MAPE, paraffin, and foamer is 100. the percentage of mMMT is a percentage of the total amount.

FTIR analysis of modified montmorillonite

The group changes before and after MMT modification were measured by Fourier transform infrared spectrometer (Magna-IR560; Thermo Nicolet Corporation, Madison, WI, USA). The tested samples were mixed with KBr powder and pressed into thin wafers for testing. The wavenumber scanning range was from 4000 cm^{-1} to 500 cm^{-1}, the resolution was 4 cm^{-1}, and the number of scans was 32.

Micromorphological analysis

Scanning electron microscopy (SEM) works on the basis of interaction between electrons and matter. That is, when a beam of high-energy incident electrons strikes the surface of a substance, the interaction between electron and substance is used to obtain a variety of physical and chemical information of each sample. During the test, the sample was prepared into small lumps with a cutter, and the section facing upward was made flat. Each sample was placed on the sample holder, both sides of the sample were glued with conductive carbon adhesive, and then the gold film was evaporated and sprayed in a vacuum coating machine (FEI Company, Hillsboro, OR, USA). The experimental process was tested in accordance with ASTM E1588 (2017). Morphology and characteristics of scanning electronic micro lens FEI QUANTA200 (FEI Company, Hillsboro, OR, USA) were observed at an accelerated voltage of 30 kV.

Mechanical sample preparation and performance test

The prepared mMMT/PP/wood fiber foam composite material was sawn into a standard test piece by a precision table saw (HW110L-50; Hongrui Precision Cutting Tools Co., Ltd., Dongwan, China) and a dumbbell-type sampler (BGD-5102; Bogda Testing Instrument Co., Ltd., Qingdao, China). There were 6 test pieces per group, wherein the impact test piece size was 80 mm × 10 mm × 4 mm, bending sample size was 80 mm × 13 mm × 4 mm, and tensile sample size was 165 mm × 20 mm × 4 mm). Bending performance was tested according to ASTM D790 (2010), tensile performance was tested according to ASTM D638 (2010), and impact performance was tested according to ASTM D256 (2010).

The impact test method of plastics only supported beams showed that the test results were the arithmetic average of five samples. Mechanical strength of the test piece was measured with a WDW-20 electronic universal testing machine (Changchun Kexin Test Instrument Co., Ltd., Jilin, China) and observed with a scanning electron microscope (SEM-EDXA; FEI Company, Hillsboro, OR, USA) equipped with an energy spectrometer. Roughness and cracking degree of cross-section of the test piece were used to characterize microscopic morphology, such as size and uniformity of foam voids.

Shrinkage sample preparation and testing

The mixture of 67% PP, 27% wood powder, and 3% MAPE, 1% paraffin, 2% foamer ADC, and different amounts of mMMT were mixed with a high-mixer (GHV type; Tianjin Saide Electronic Control Machinery Equipment Co., Ltd., Tianjin, China). The mixture was obtained by extrusion granulation through a twin-screw extruder to obtain a raw material for injection molding, and then it was injection molded into a standard shrinkage test piece by a RPWXZSJ-8100 micro-injection molding machine (Shanghai Runpin Teaching and Research Center, Shanghai, China). Cylinder temperature was 185 °C, nozzle temperature was 200 °C, injection pressure was 75 MPa, holding pressure was 70MPa, pressure holding time was 10 s, and injection speed was 40cm^3/s. The standard sample size was 80 mm × 10 mm × 4 mm. After stripping, the sample was placed at 23 °C ± 2 °C for 6 h to 24 h, and then the size of the spline was measured by Cpj-3020a / AZ Marriott projector (Yifeng Xintian Precision Instrument Co., Ltd., Suzhou, China). The experiment was conducted according to ASTM D2732 (2008) and Eq. 1 is as follows,

$$SM_P = 100(L_0 - L_1)/L_0 \tag{1}$$

where SM_P is the molding shrinkage (%), L_0 is the cavity length (mm), and L_1 is the sample length (mm).

Sample preparation and testing of hygroscopic properties

According to the determination method ASTM D570-98 (2018), a SZ-3 panel saw machine (Hongrui Precision Cutting Tools Co., Ltd., Dongwan, China) was used to prepare mMMT/foam-wood-plastic composite material into a hygroscopic preparation absorption sample. The size of the sample was 10 mm × 10 mm × 4 mm. The hygroscopic sample was placed in a constant temperature drying box at 103 °C until dry before the absorption experiment.

The chemical reagent (Na_2SO_4) was separately placed into dryers to prepare a saturated solution with a relative humidity of 93%. The indoor environment temperature was 20 °C. Then, each sample was placed in the corresponding dryer according to target relative humidity. Finally, vaseline was used to seal and store until saturation state. The test results were the averages of eight samples. After the sample reached equilibrium, sample weight was recorded as W_t, and then the sample was dried in a drying box at 103 °C until it reached an absolute dry state. At this time, sample weight was recorded as W_0, and equilibrium moisture content of the sample was calculated as shown in Eq. 2,

$$EMC\ (\%) = [(W_t - W_0)\ /\ W_0] \times 100 \tag{2}$$

where EMC is the equilibrium water content of the sample (%), W_0 is the absolute dry weight of samples (g), and W_t is the weight of sample after treatment (g).

RESULTS AND DISCUSSION

Preparation of Modified Montmorillonite

The MMT and silane coupling agent were prepared with a mass ratio of 100:4, fully mixed in a high-speed mixing machine with a temperature of 60 °C, and then dried at 80 °C for 6 h to obtain mMMT. The FTIR test showed that the basic framework of mMMT infrared spectrum did not change, and a new absorption peak appeared between 2838 and 3102 cm^{-1}, which indicated that the coupling agent had been adsorbed on the surface of MMT particles.

FTIR Analysis

Figure 3 shows the infrared spectra of untreated wood fiber surface and modified wood fiber surface with impulse and cyclone high temperature treatment. Compared with untreated wood fiber (curve a), intensity of OH^{-1} absorption peak at 3430 cm^{-1} and C=O absorption peak at 1738 cm^{-1} in modified wood fiber decreased, among which the hydroxyl absorption peak decreased remarkably. Xuan *et al*. (2017) also reported that surface-modified TiO_2 nanoparticles on the anti-ultraviolet aging performance of wood-based Foamed Composites. For the A171-treated TiO_2 (curve-4b), the broad absorption peak between 3400 cm^{-1} and 3200 cm^{-1} was weakened, and for the peak at around 1630 cm^{-1}, the research results were similar. Under impact of impulse and cyclone high temperature treatment, free hydroxyl groups in molecular chains of wood cellulose had a "bridging" reaction with each other, and ether bonds were generated, which noticeably reduced the number of free hydroxyl groups on the surface of wood fiber. In addition, under impact of impulse and cyclone high temperature treatment, hemicellulose had a

drastic degradation reaction, the acetyl group in hemicellulose was detached, and acetic acid was produced by hydrolyzation, which resulted in reduction of the number of carbonyl groups C=O.
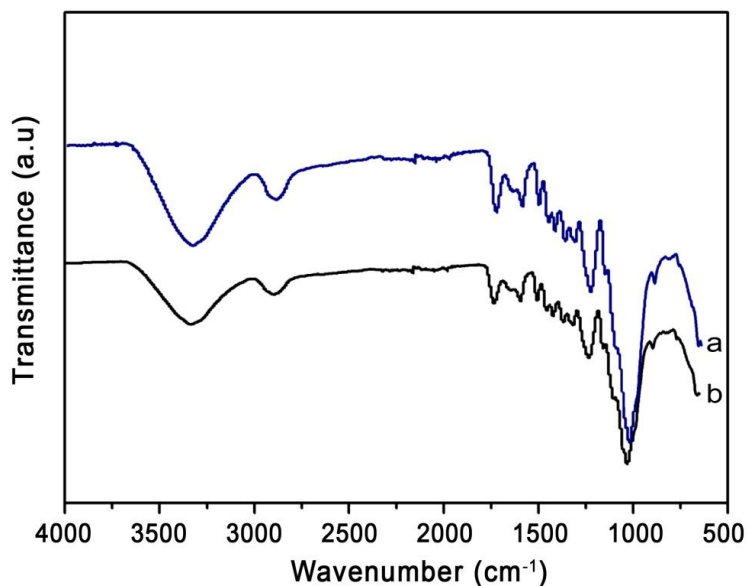

Fig. 1. Comparison of FTIR spectra obtained for wood fibers modified through impulse and cyclone high temperature treatment under different conditions: (a) untreated and (b) impulse-cyclone high temperature treatment, *T* = 220 °C

Effect of Modified Montmorillonite on Surface Microstructure of Wood-based Foamed Composites

When modified montmorillonite/polypropylene/wood fiber foam composite was prepared using azodicarbonamide foamer, nitrogen gas was released and foamed. The foaming was relatively high, and the nucleation of bubbles was also good. Due to the hot-pressing process, the surface of the material formed a hard skin due to drastic cooling, and pores were mostly formed inside the composite material. Bubble nucleation effects mainly have two cases: one is a composite material with a great amount of matrix in the bubble hole (Moscoso-Sánchez *et al.* 2013). In this case, the bubble holes were evenly distributed, and the pore-forming effect was better. The nucleation frequency was high as well. Therefore, under the effect of azobisformamide foamer, in modified montmorillonite/PP/wood fiber composite matrix, the sizes of bubble holes were evenly distributed with a small diameter and uniform distribution. The matrix composite materials formed high-quality foam. Nevertheless, an improper amount of azodicarbonamide foaming agent will lead to poor nucleation behavior of the foam in the composite matrix, which was improper azobisformamide dosage of foamer leading to poor the pore-forming effect in the composite matrix (Babaei *et al.* 2014). The bubble nucleation was not produced at the same time. Under action of azobisformamide, in the process of heating, air bubble nucleation formed step-by-step, which caused too large or too small of bubble hole sizes, unstable bubble hole density, and uneven distribution. Finally, the foaming matrix became an inferior foamer.

When the amount of mMMT added was 0 wt%, distribution of cells on the fracture surface of sample 1 was observed by SEM. Foaming was uniform in the fracture surface, the fracture caused breakage of PP and wood fibers, and fracture occurred mostly

in the cells. In the gap of the cells, fracture of wood fiber was clearly visible. Fracture of wood fiber, PP, and wood fiber carried most of the destructive force. The phenomenon where wood fiber was pulled out in the cell was good, and wood fiber was well-received by HDPE. The package was not exposed to the inner wall of the cell, which indicated that foamer ADC effectively foamed the PP (Faruk *et al.* 2007).
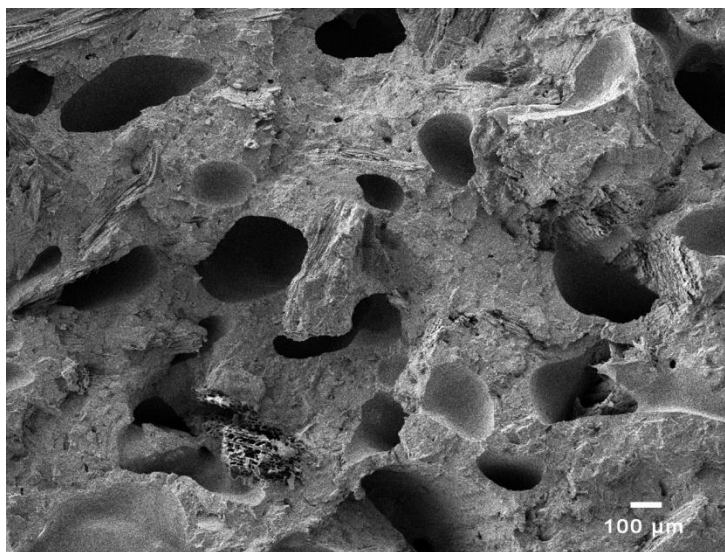
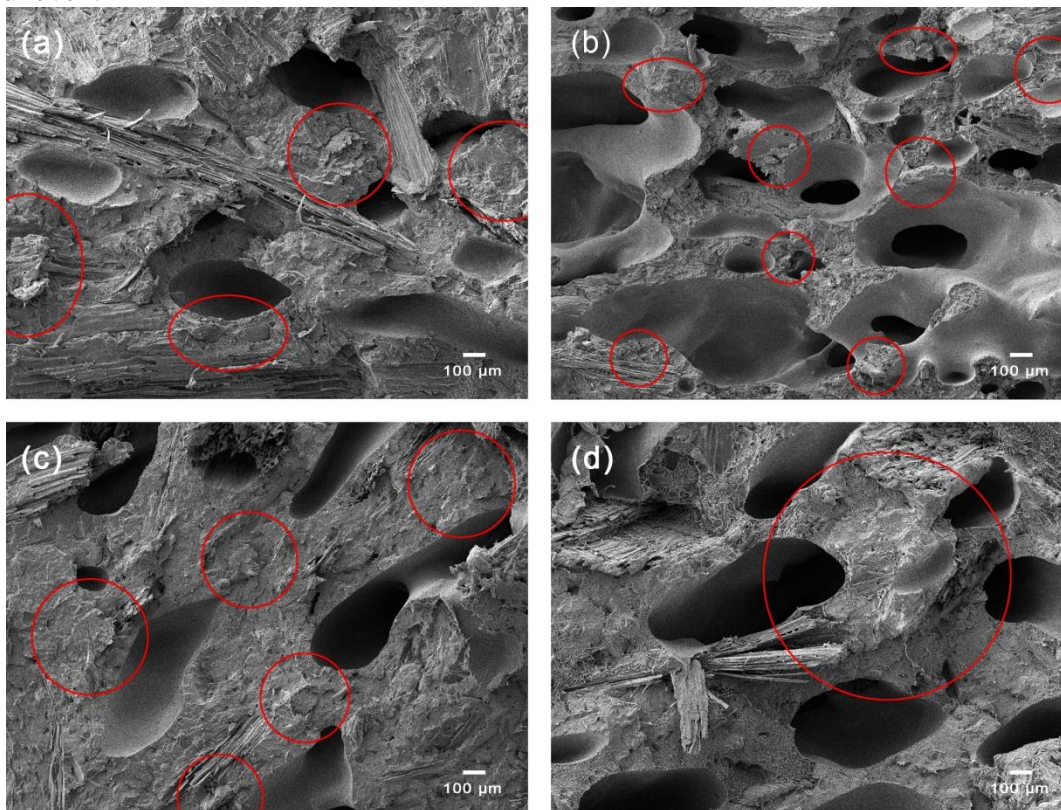**Fig. 2.** SEM image of wood-based foaming composites with mMMT-0

Figure 3 shows the electron microscope image of mMMT/PP/wood fiber foamed composite. As shown in Fig. 3(a), mMMT reinforcement was 3wt%. When the fracture surface of sample 2 with SEM was observed, bubble holes were evenly distributed. Distribution of mMMT appeared on the larger fracture surface between bubbles, and wood removal fibers and plastics that bore the destructive force were not affected by bubbles. At the same time, mMMT distributed in the bubble gap was transformed into the supporting structure of the material and played a further bonding role.

As shown in Fig. 3(b), when the fracture surface of sample 3 was observed by SEM under 100X, it was found that in sample 3 with 5 wt% mMMT reinforcement, the the number of bubble holes increased, and mMMT was evenly distributed in the gap of bubble holes. In mMMT/PP/wood fiber foamed composites, mMMT and wood fiber together formed the framework of material and played a good supporting role. Because diameter of wood fiber (40-mesh > d ≥ 60-mesh) was longer than that of mMMT particle (80-mesh), mMMT with hard texture and small particle size filled in gaps of wood fibers, but they were well-wrapped by PP and were not exposed to the inner wall of blister holes, which maximized the binding effect of mMMT.

As shown in Fig. 3(c), mMMT reinforcement reached 7 wt%, the bubble hole of foamed composite material decreased slightly, and diameter of the bubble hole began to decrease to approximately 120 μm. Wood fiber and mMMT constituted the framework of foaming material, because too much mMMT led to mixing and dispersion of wood fiber and PP, and PP could not play a good role in packaging. The small portion of mMMT was exposed to the inner wall surface of the bubble hole, which resulted in the decrease of reinforcing effect of mMMT and mechanical properties of mMMT/PP/wood fiber foamed composites.

As shown in Fig. 3(d), mMMT reinforcement increased to 10 wt%. When fracture surface of sample 5 was observed by SEM, it was found that the bubble hole became uneven.

Fig. 3. 100X SEM images of wood-based foaming composites with different amounts of mMMT: (a) 3 wt% mMMT, (b) 5 wt% mMMT, (c) 7 wt% mMMT, and (d) 10 wt% mMMT

The agglomeration phenomenon of mMMT was observed at 100X. The mMMT contained SiO_2, Al_2O_3, MgO, and other minerals. Energy spectrum analysis showed that the composition inside the red area was mostly SiO_2 Al_2O_3, MgO, and other mineral compositions. It could be determined that the material inside the red point in the picture was mMMT, as shown in Fig. 4.
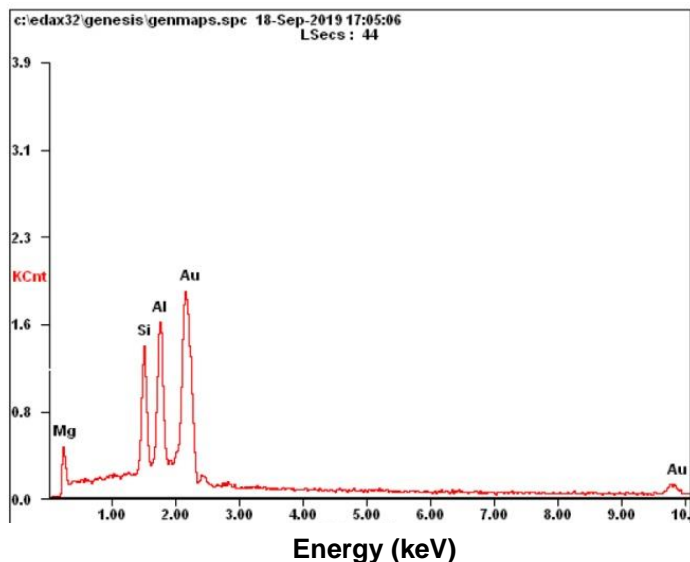
Fig. 4. Spectrum from Energy analysis of wood-based foaming composites

The fracture surface of sample 2 with SEM was observed. When mMMT reinforcement was 3 wt%, bubble holes were evenly distributed than other samples as shown form Fig. 3. The chemical composition was fine, at approximately 0.2 μm to 1 μm. Reinforcement of mMMT particles was below 187.5 μm. The mMMT contained aquifer-like silicate minerals that belonged to a monoclinic system. These components have colloidal dispersion characteristics and are usually aggregated in bulk or soil under their own flocculation. Due to excessive mMMT reinforcement, agglomerated clay blocks were full of bubbles, and mMMT was largely exposed to the inner wall surface of bubbles, which affected the mixed contact surface between wood fiber and PP, destroyed the wrapping effect of PP, and finally led to further decline of mechanical properties of foamed composites.

In summary, azodicarbonamide foamer was used to prepare modified montmorillonite/polypropylene/wood fiber foaming composite. The mass ratio of foamer and substrate was 2:100. An electric sulfur adding molding machine was used to mold raw material particles by hot-pressing, and the temperature was set at 180 °C, which could effectively improve nucleation density and nucleation of bubbles, which made the matrix filler melt quickly. Preloading for 15 min made azodicarbonamide foamer dissolve and disperse well in polypropylene/wood fiber melt, which improved nucleation of bubbles. At the same time, modified montmorillonite was integrated into the melt again, which formed a "bridging" effect with polypropylene. When matrix filler was fixed at 100 g, final volume and size of polypropylene/wood fiber melt were quantified, which further improved nucleation density and bubble hole density. The cold-pressing method performed for 5 min made the melt surface form hard skin rapidly. Then, the melt was finalized, and modified montmorillonite was integrated into the pore wall of the foam hole, which formed a skeleton supporting function and further enhanced mechanical properties of foamer WPCs. The mMMT/PP/wood fiber foamed composites with reinforcement of 5 wt% mMMT and 2 wt% azodicarbonamide foamer had the best properties.

Effect of Modified Montmorillonite on Mechanical Properties of Wood-based Foamed Composites

As shown in Table 2, mMMT reinforcement effectively enhanced mechanical properties of foamed wood-plastic composites. Reinforcements of mMMT in the samples were 0 wt%, 3 wt%, 5 wt%, 7 wt%, and 10 wt%, respectively. According to the comparison of mechanical properties of the samples, reinforcement performances of mMMT were as follows: flexural strength was from 19.73 MPa to 27.53 MPa, bending elastic modulus was 1229.89 MPa to 2112.04 MPa, tensile strength was from 11.68 to 19.95 MPa, fraction elongation was from 2.67 to 1.86%, and impact strength was from 3.52 KJ/m^2 to 6.30 KJ/m^2.

Flexural strength and impact strength of sample 3 improved. Compared with sample 3, flexural strength, tensile strength, and elongation at break of sample 5 decreased. It was found that there was more mMMT in sample 5 than sample 3 by SEM. The mMMT was largely exposed to the inner wall surface of bubbles, destroyed the wrapping effect of PP, and finally led to further decline of mechanical properties of foamed composites.

Table 2. Mechanical Properties of Wood-based Foaming Composites

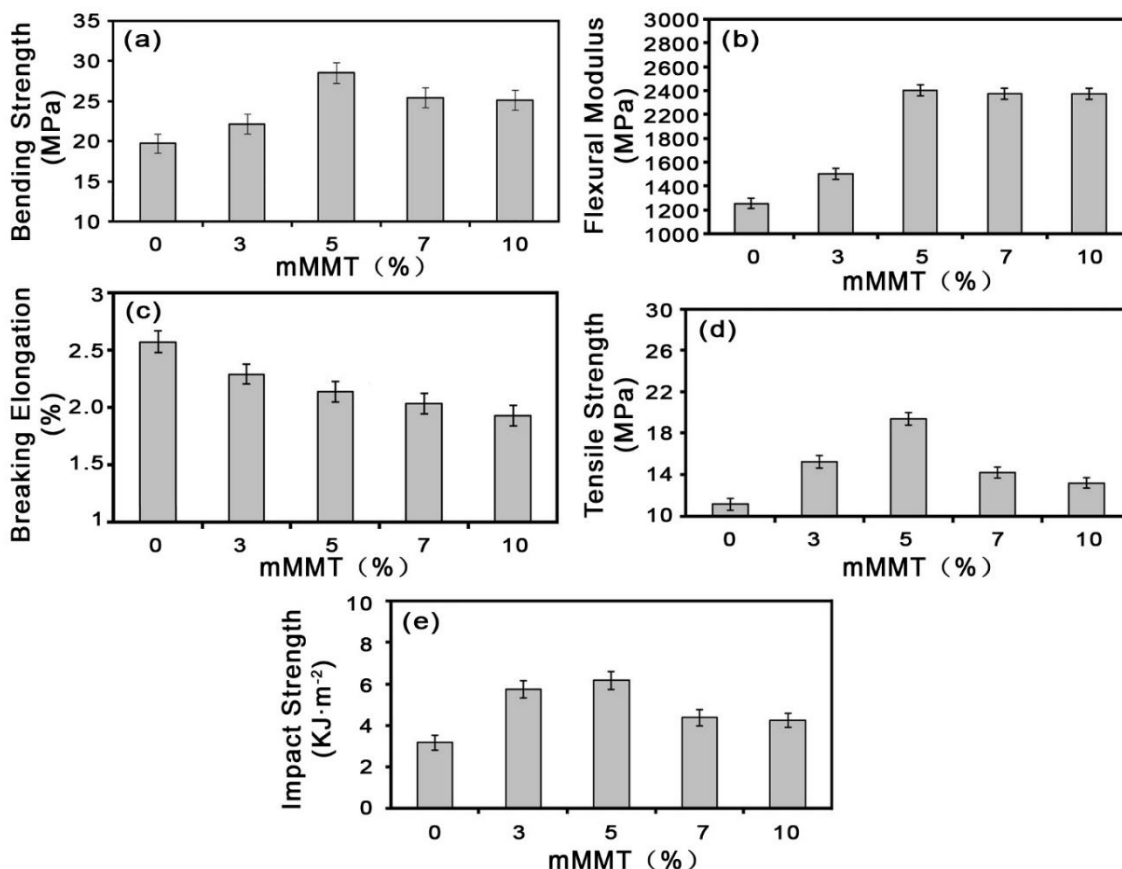| Sample No.	Flexural Strength (MPa)	Flexural Modulus (MPa)	Elongation at Break (%)	Tensile Strength (MPa)	Impact Strength (KJ/m^2)
1	19.73±0.98	1229.89±27.48	2.67±0.23	11.68±0.83	3.52±0.41
2	23.36±0.93	1554.38±26.26	2.34±0.24	16.61±1.25	5.91±0.64
3	27.53±0.85	2112.04±21.95	2.19±0.19	19.95±1.56	6.30±0.71
4	25.86±1.16	1924.27±23.37	2.05±0.15	14.95±1.32	4.34±0.54
5	25.54±1.25	1921.40±25.59	1.86±0.18	13.68±1.55	4.27±0.50

As shown in Figs. 5(a) and 5(b), both flexural strength and flexural modulus of sample 3 showed an upward trend. The maximum flexural strength reached 27.5 MPa, with an increase of 7.8 MPa, which represents a 28.3% increase. It was indicated that reinforcement of 5 wt% mMMT increased bearing pressure in the compression area above the rectangular uniform section of the sample, and tensile resistance in the tensile area below the section also increased. In the process of wood fiber and plastic bonding, mMMT played the role of strengthening the matrix of foamed composite material. Flexural strength of sample 5 began to show a downward trend, decreasing 1.99 MPa (7.2%). This showed that more than 5 wt% mMMT exhibited an agglomeration phenomenon, which played an obstacle role in the composite process of wood fiber and PP, leading to a decline in flexural strength. When mMMT reinforced quantity reached 5 wt%, the bending modulus of sample 3 rose and bent easily.

As shown in Fig. 5(c), when mMMT reinforcement reached 5 wt%, elongation at break of sample 3 decreased 1.0%, with a decline of 12.2%. There was little change in tensile strength or elongation at break for this occasion. When mMMT reinforcement exceeded 5 wt%, the elongation at break of sample 4 and sample 5 showed a decreasing

bioresources.com

trend. Such variation law indicated that when mMMT reinforcement was too much, it could not bond well with wood fiber. When mMMT reinforcement reached 10 wt%, the decrease in amplitude was 14.20%. As a result, stress-bearing capacity of the matrix was reduced, and a large number of bubble holes occupied the matrix of the material, which resulted in a decline in absolute compactness volume and tensile area of the matrix, making it fracture under relatively small tensile force. Compared with sample 1, bending modulus of sample 5 increased 882 MPa, with an increase percentage of 41.8%. When mMMT reinforcement reached 10 wt%, bending modulus of sample 5 decreased to 1921 MPa, and still increased by 692 MPa compared with sample 1. This showed that mMMT/PP/wood fiber foamed composites were prone to bend and deform under bending stress. When bending deformation occurred, foamed composites occupied part of the volume space of the material, which led to deformation, reduced brittleness, and increased toughness of the matrix (Ghasemi *et al.* 2012). The role of mMMT in reinforcing the matrix also played an important role, which made the wood foam. The elastic limit of composites was further improved.

As shown in Fig. 5(d), tensile strength increased first and then decreased as the amount of mMMT was increased. When mMMT reinforcement reached 5 wt%, tensile strength of sample 3 reached 20.0 MPa, with an increase of 41.4%. When mMMT reinforcement exceeded 5 wt%, tensile strength of sample 4 and sample 5 showed a decreasing trend, which indicated that when mMMT reinforcement was too high, PP and wood fiber could not bond well, and this led to a decrease in stress-bearing capacity of the substrate, where mMMT caused it to fracture under relatively small tensile force.

As shown in Fig. 5(e), when mMMT reinforcement was 5 wt%, impact strength of sample 3 reached the maximum value of 6.30 KJ/m^2, which increased 2.78 KJ/m^2 compared with that of sample 1, with an increase of 44.1%. This indicated that mMMT was better filled between PP and wood fiber, which resulted in the bonding effect. When impact force was received, there were many cracks on the surface that absorbed a large amount of impact energy and thereby improved impact resistance of wood-based foamed composites. When mMMT reinforcement reached 10wt%, impact strength of sample 5 decreased to 4.27 KJ/m^2, with a decrease of 32.2%. The main reason was that the impact process mainly absorbed impact force through generation and expansion of cracks. When too much mMMT was added, its reinforcement was too high, and mMMT was prone to the phenomenon of uneven dispersion, agglomeration, and other phenomena, and was exposed to the inner wall of the bubble hole, resulting in a decline of impact capacity of the hole wall, and impact strength decreased instead of increasing.

Fig. 5. Effects of amount of mMMT added on mechanical properties of wood-based foaming composites: (a) flexural strength, (b) flexural modulus, (c) elongation at break, (d) tensile strength, and (e) impact strength

After comprehensive consideration, different proportions of mMMT were filled in wood-based foamed composites, and mechanical properties were tested as follows: with the increase of filling amount of mMMT, flexural strength, flexural modulus, tensile strength, and impact properties of mMMT/PP/wood fiber foamed composite showed a trend of first increasing and then decreasing, and elongation at break showed a decreasing trend. Mechanical properties of mMMT/PP/wood fiber foamed composites were optimized when mMMT reinforcement was 5 wt%.

Effect of Modified Montmorillonite on Shrinkage and Porosity of Wood-based Foamed Composites

Table 3 shows the effect of mMMT on porosity and shrinkage of wood-based foaming composites. Reinforcement of mMMT in the samples 1 through 5 were 0 wt%, 3 wt%, 5 wt%, 7 wt%, and 10 wt%, respectively. When mMMT/PP/wood fiber foamable composite samples were prepared with a thezs-406b electric sulfur-adding molding machine, the packing mass was 100 g and volume of the hot-pressing mold was 15cm×15cm×0.4cm. Absolute compacted volume of the sample was measured by Eq. 3 (Xi *et al.* 2017):

$$Porosity\ (\%) = \frac{(Apparent\ volume\ 160) - (Absolute\ compacting\ volume)}{Apparent\ volume} \times 100\% \qquad (3)$$

bioresources.com

Injection material was obtained using the twin-screw extruder, and then it was injected into the standard shrinkage sample by the RPWXZSJ-8100 micro-injection molding machine. The standard sample was placed in an oven to be dried for 2 h, and then dried at a constant temperature of 23 °C for 48 h after being removed. The length of the spline was measured with a measuring projector. The size (mm) of the plastic part was recorded as M, length (mm) of the mold was recorded as D, and absolute shrinkage (%) of material was recorded as S. Shrinkage and porosity of mMMT reinforced wood-based foamed composites were calculated by Eq. 1 and Eq. 3, as shown in Table 3.

Table 3. Effects of Amount of mMMT Added on Shrinkage and Porosity of Wood-Based Foaming Composites

Sample No.	Absolute Compacting Volume (cm^3)	Shrinkage (%)	Porosity (%)
1	70.86±2.01	1.35±0.15	21.25±2.76
2	70.82±2.08	1.26±0.11	21.31±2.40
3	70.75±2.12	1.17±0.09	21.39±2.58
4	71.33±2.16	1.22±0.10	20.75±2.16
5	73.38±2.23	1.28±0.12	18.47±2.02

Table 3 shows that foamed wood-plastic composite reinforced by mMMT was determined by the proportion of each component. When mMMT reinforcement was 5 wt%, absolute compacted volume value of sample 3 was 70.8 cm^3, porosity reached 21.4%, and shrinkage was only 1.17%. Although porosity was high, shrinkage was lowest in the preparation process, which led to the largest bubble hole and even foaming. With the increase of mMMT reinforcement, the absolute compatibility volume value corresponding to mMMT/PP/wood fiber foamed composite showed an overall trend of increasing, with the maximum increasing range of 73.4 cm^3. The trend of porosity was opposite to that of absolute compacting volume value. When absolute compacting volume value increased, porosity correspondingly decreased.

The mMMT used for strengthening wood-based foamed composites was approximately 80-mesh with small particles. After extrusion, mMMT particles of MMT reinforced wood-plastic composites were filled in the pores of wood fiber, which resulted in a decrease in porosity and a rise in density of PP/wood-fiber foamed composites. Ceramic structure was changed, and hardness increased at high temperature. While increasing the support strength of wood-based foamed composite skeleton, it also promoted shrinkage of material. Therefore, mMMT/PP/wood fiber foam composite with enhanced mMMT had a higher absolute volume value and a lower shrinkage ratio, and absolute compact volume value was inversely proportional to shrinkage ratio.

Effects of Modified Montmorillonite on Water Absorption and Thickness Swelling of Wood-based Foamed Composites

Water absorption test

Figure 6 shows the effect of different mMMT reinforcements on water absorption of wood-based foaming composite materials. The mMMT reinforcements for the samples were 0 wt%, 3 wt%, 5 wt%, 7 wt%, and 10 wt%, respectively. Water absorption of

mMMT/PP/wood fiber foam composite was caused by a large number of cavities, foam holes, and hydroxyl and polar groups in the wood fiber foam composite, as well as some cracks and gaps between wood fiber and resin matrix interface. Compared with sample 1 with no reinforced mMMT, after reinforced mMMT foamed wood-plastic composite materials, the water absorption of the other samples first increased and then decreased with the increase of the added amount. Among them, bibulous absorption of sample 3 (mMMT) 5 wt% increased the most noticeably. Equilibrium water absorption was 9.28%, which was 5.14% higher than that of sample 1 (4.14%) without reinforcing mMMT.
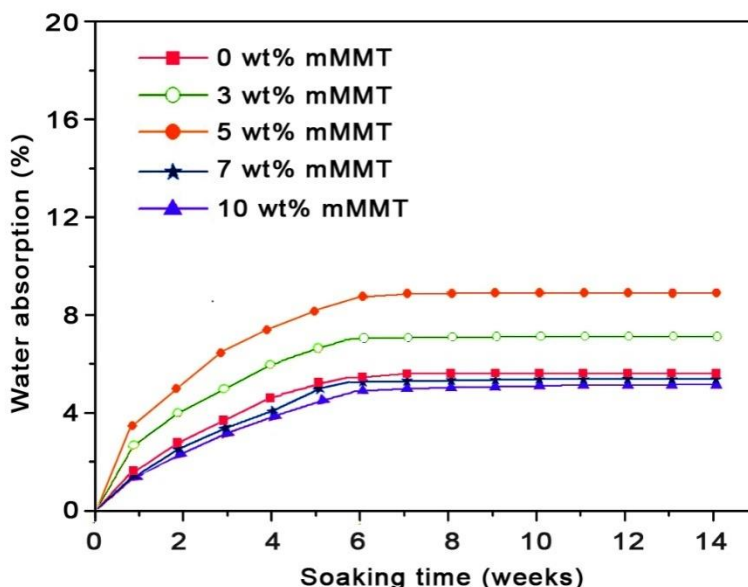

Fig. 6. Water absorption of wood-based foaming composites with different amounts of mMMT

During the experiment, with the increase of soaking time of samples, water absorption of both wood-based foam composites without mMMT and composites with mMMT noticeably increased, and water absorption of composite material reached a balance after 10 weeks, and water absorption of the wood-based foam composite increased remarkably at the beginning of the sample experiment (0 weeks to 6 weeks). Under treatment of silane modifier, hydroxyl on the surface of mMMT reacted with silane coupling agent, which led to decreases of hydroxyl number, polarity, and water absorption. In addition, in the mixing process, wood fiber was packed by mMMT and PP and further blocked contact between wood fiber and water so that water absorption of wood fiber was reduced. When mMMT reinforcement was 5 wt%, the mixture was the most even, the bubble hole diameter produced inside the material was the largest, and its water absorption was the highest. When mMMT reinforcement was too high, mMMT appeared to demonstrate agglomeration phenomenon, which produced even foam holes. Diameter of foam holes decreased, leading to decreased water absorption.

Thickness swelling test

Figure 7 shows the influence of different mMMT reinforcements on thickness swelling of mMMT/PP/wood fiber foam composite material. The mMMT reinforcements of samples 1 through 5 were 0 wt%, 3 wt%, 5 wt%, 7 wt%, and 10 wt%, respectively. Compared with sample 1, with increased soaking time of samples, thickness swelling of

foam wood-plastic composites both without mMMT and with mMMT noticeably increased, and they reached a balance after 10 weeks. The thickness swelling of samples at the beginning of the experiment (0 weeks to 6 weeks) was higher. Among them, thickness swelling of foamed wood-plastic composites with 5 wt% mMMT reinforcement decreased the most remarkably, with a decrease of 25%.
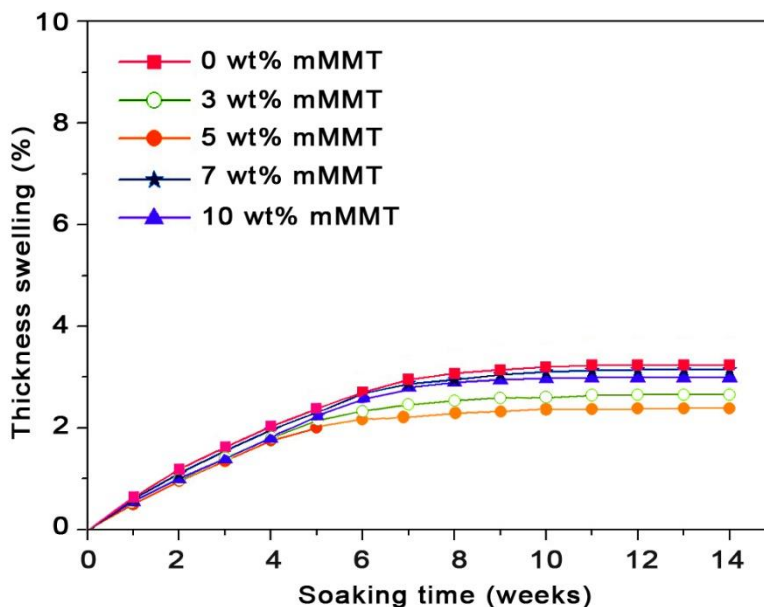

Fig. 7. Thickness swelling of wood-based foaming composites with different amounts of mMMT

Because thickness swelling of foamed wood-plastic composite increased with the increase of water absorption, it had a similar trend with water absorption. Wood fibers and mMMT constituted the framework of foaming materials. When mMMT reinforcement was too high, it led to mixing and dispersion of wood fiber and PP, and PP could not play a big role in wrapping. This led to decreases in strength of the foam material itself, and wood fiber that would be exposed to the outside and expand after absorbing water, leading to the uneven surface of the sample and the increase of thickness swelling.

CONCLUSIONS

1. The research results showed that reinforcement with a certain amount of mMMT could effectively improve performance of wood-based foam composite and enhance skeleton support function of wood-based foam composites. However, when the amount of reinforcement was excessive, the enhancement effect showed a downward trend.

2. Azodimethylamide foamer released nitrogen at 180 °C and foamed. Due to the hot-pressing process, the surface of the material was hard because of drastic cooling, and the pores were mostly formed in the interior of the composite material.

3. The SEM observation showed that bubble holes increased in the fracture surface of sample 3 with 5 wt% mMMT reinforcement, which was observed at 100X.

Additionally, MMT was evenly distributed in the cell gap and was well-encapsulated by PP, but not exposed to the inner wall of the cell. The bonding effect of mMMT was maximized. When mMMT reinforcement increased to 10 wt%, bubble holes in the fracture surface became uneven. The mMMT agglomeration was then observed at 100X. With mMMT being largely exposed to the inner wall surface of foam holes, the mixing contact surface between wood fiber and PP was affected, which destroyed the wrapping function of PP, and finally led to further decline in mechanical properties of foamed composites.

4. Mechanical property test results showed that flexural strength was 27.5 MPa and the increase was 28.3% when mMMT reinforcement was 5 wt%. Flexural modulus increased by 41.8% to 2110 MPa. Breaking elongation decreased 12.2% to 2.2% of original length. Tensile strength was 20.0 MPa with an increase of 41.5%. Impact strength was 6.30 KJ/m^2, with an increase of 44.1%. The increase was obvious, and mechanical properties of wood-based foamed composites were effectively optimized. When mMMT reinforcement exceeded 5 wt%, mechanical properties began to decline and elongation at break presented a consistent trend of decline.

5. The shrinkage and porosity tests showed that when mMMT reinforcement was 5 wt%, absolute density volume value of wood foam composite was 70.8 cm^3, porosity was 21.4%, and the shrinkage was 1.17%. Absolute density volume value was inversely proportional to shrinkage. The test of water absorption and thickness swelling showed that when mMMT reinforcement was 5 wt%, water absorption of foam composite increased noticeably, equilibrium water absorption was 9.28%, with an increase of 5.14%. Thickness swelling decreased remarkably by 25%. When mMMT reinforcement exceeded 5wt%, the water absorption decreased, while the thickness swelling increased.

ACKNOWLEDGMENTS

Author Contributions
Qingde Li and Feng Chen conceived of, designed, and performed the experiments. Qingde Li, Yingyi Liang, and Tonghui Sang analyzed and discussed the data. Qingde Li wrote the manuscript, with revisions by Feng Chen.

REFERENCES CITED

ASTM D256 (2010). "Standard test methods for determining the Izod pendulum impact resistance of plastics," ASTM International, West Conshohocken, PA, USA.
ASTM D570-98 (2018). "Standard test method for water absorption of plastics," ASTM International, West Conshohocken, PA, USA.
ASTM D638-10 (2010). "Standard test method for tensile properties of plastics," ASTM International, West Conshohocken, PA, USA.

ASTM D790-10 (2010). "Standard test methods for flexural properties of unreinforced and reinforced plastics and electrical insulating materials," ASTM International, West Conshohocken, PA, USA.

ASTM D2732-08 (2008). "Standard test method for unrestrained linear thermal shrinkage of plastic film and sheeting," ASTM International, West Conshohocken, PA, USA.

ASTM E1588-17 (2017). "Standard practice for gunshot residue analysis by scanning electron microscopy/energy dispersive X-ray spectrometry," ASTM International, West Conshohocken, PA, USA.

Babaei, I., Madanipour, M., Farsi, M., and Farajpoor, A. (2014). "Physical and mechanical properties of foamed HDPE/wheat straw flour/nanoclay hybrid composite," *Compos. Part B- Eng.* 56, 163-170. DOI: 10.1016/j.compositesb.2013.08.039

Bledzki, A. K., and Faruk, O. (2006). "Injection moulded microcellular wood fibre–polypropylene composites," *Compos. Part A-Appl. S.* 37(9), 1358-1367. DOI: 10.1016/j.compositesa.2005.08.010

Choi, N.-W., Mori, I., and Ohama, Y. (2006). "Development of rice husks–plastics composites for building materials," *Waste Manage.* 26(2), 189-194. DOI: 10.1016/j.wasman.2005.05.008

Ding, D., Li, P., Zhang, X., Ramaswamy, S., and Xu, F. (2019). "Synergy of hemicelluloses removal and bovine serum albumin blocking of lignin for enhanced enzymatic hydrolysis," *Bioresource Technol.* 273, 231-236. DOI: 10.1016/j.biortech.2018.11.024

Faruk, O., Bledzki, A. K., and Matuana, L. M. (2007). "Microcellular foamed wood‐plastic composites by different processes: A review," *Macromolecular Materials and Engineering* 292(2), 113-127. DOI: 10.1002/mame.200600406

Gamelas, J. A. F., and Ferraz, E. (2015). "Composite films based on nanocellulose and nanoclay minerals as high strength materials with gas barrier capabilities: Key points and challenges," *BioResources* 10(4), 6310-6313. DOI: 10.15376/biores.10.4.6310-6313

Gao, Z., Huang, R., Chang, J., Li, R., and Wu, Y. (2019). "Effects of pressurized superheated-steam heat treatment on set recovery and mechanical properties of surface-compressed wood," *BioResources* 14(1), 1718-1730. DOI: 10.15376/biores.14.1.1718-1730

Ghasemi, I., Farsheh, A. T., and Masoomi, Z. (2012). "Effects of multi-walled carbon nanotube functionalization on the morphological and mechanical properties of nanocomposite foams based on poly (vinyl chloride)/(wood flour)/(multi-walled carbon nanotubes)," *Journal of Vinyl and Additive Technology* 18(3), 161-167. DOI:10.1002/vnl.20299

Han, Y., Manolach, S. O., Denes, F., and Rowell, R. M. (2011). "Cold plasma treatment on starch foam reinforced with wood fiber for its surface hydrophobicity," *Carbohyd. Polym.* 86(2), 1031-1037. DOI: 10.1016/j.carbpol.2011.05.056

Jonasson, S., Bünder, A., Niittylä, T., and Oksman, K. (2019). "Isolation and character-ization of cellulose nanofibers from aspen wood using derivatizing and non-deriva-tizing pretreatments," *Cellulose* 27(1),1-19. DOI: 10.1007/s10570-019-02754-w

Kallakas, H., Ayansola, G. S., Tumanov, T., Goljandin, D., Poltimäe, T., Krumme, A., and Kers, J. (2019). "Influence of birch false heartwood on the physical and mechanical properties of wood-plastic composites," *BioResources* 14(2), 3554-3566. DOI: 10.15376/biores.14.2.3554-3566

Matuana, L. M., Park, C. B., and Balatinecz, J. J. (1997). "Processing and cell morphology relationships for microcellular foamed PVC/wood-fiber composites," *Polym. Eng. Sci.* 37(7), 1137-1147. DOI: 10.1002/pen.11758

Okon, K. E., and Udoakpan, U. I. (2019). "Physicochemical properties of *Pinus massoniana* wood subjected to silicone oil heat treatment," *Maderas- Cienc. Tecnol.* 21(4), 531-544. DOI: 10.4067/S0718-221X2019005000409

Petchwattana, N., and Covavisaruch, S. (2011). "Influences of particle sizes and contents of chemical blowing agents on foaming wood plastic composites prepared from poly(vinyl chloride) and rice hull," *Mater. Des.* 32(5), 2844-2850. DOI: 10.1016/j.matdes.2010.12.044

Sun, Z., and Wu, M. (2019). "Effects of sol-gel modification on the interfacial and mechanical properties of sisal fiber reinforced polypropylene composites," *Ind. Crop. Prod.* 137, 89-97. DOI: 10.1016/j.indcrop.2019.05.021

Wang, W., Sain, M., and Cooper, P. A. (2005). "Hygrothermal weathering of rice hull/HDPE composites under extreme climatic conditions," *Polym. Degrad. Stabil.* 90(3), 540-545. DOI: 10.1016/j.polymdegradstab.2005.03.014

Wang, Q., Xiao, S., and Shi, S. Q. (2019). "The effect of hemicellulose content on mechanical strength, thermal stability, and water resistance of cellulose-rich fiber material from poplar," *BioResources* 14(3), 5288-5300. DOI: 10.15376/biores.14.3.5288-5300

Xi, J., Zhou, E., Liu, Y., Gao, W., Ying, J., Chen, Z., and Gao, C. (2017). "Wood-based straightway channel structure for high performance microwave absorption," *Carbon* 124, 492-498. DOI: 10.1016/j.carbon.2017.07.088

Xuan, L., Han, G., Wang, D., Cheng, W., Gao, X., Chen, F., and Li, Q. (2017). "Effect of surface-modified TiO_2 nanoparticles on the anti-ultraviolet aging performance of foamed wheat straw fiber/polypropylene composites," *Materials* 10(5), 456. DOI: 10.3390/jcm9030793

Yang, H.-S., Kim, H.-J., Son, J., Park, H.-J., Lee, B.-J., and Hwang, T.-S. (2004). "Rice-husk flour filled polypropylene composites; mechanical and morphological study," *Compos. Struct.* 63(3-4), 305-312. DOI: 10.1016/S0263-8223(03)00179-X

Yu, W., Xu, B., Fan, B., Zhang, Y., and Wang, X. (2020). "Effects of saturated steam treatment on the cell-wall mechanics and moisture sorption properties of kenaf fibers," *BioResources* 15(1), 159-171. DOI: 10.15376/biores.15.1.159-171

Zhang, H., Rizvi, G. M., and Park, C. B. (2004). "Development of an extrusion system for producing fine-celled HDPE/wood-fiber composite foams using CO_2 as a blowing agent," *Adv. Polym. Tech.* 23(4), 263-276. DOI: 10.1002/adv.20016